Knickpoint evolution in a supraglacial stream

Kamintzis, Jayne Elizabeth; Irvine-Fynn, Tristram; Holt, Thomas; Jones, John Paul Pryderi; Tooth, Stephen; Griffiths, Hywel; Hubbard, Bryn

Published in:
Geografiska Annaler: Series A, Physical Geography

DOI:
10.1080/04353676.2018.1549945

Publication date:
2019

Knickpoint evolution in a supraglacial stream

Kamintzis, J.E. [1]*, Irvine-Fynn, T.D.L.[1], Holt, T.O. [1], Jones, J.P.P. [2], Tooth, S.[1], Griffiths, H.[1] and Hubbard, B.[1]

[1]*Department of Geography and Earth Sciences, Aberystwyth University, Aberystwyth, SY23 3DB, Wales, UK.*

[2]*Deri Jones & Associates, Ltd., Llwyngwyn, Forge, Machynlleth, SY20 8RR, Wales, UK.*

* Email: jek12@aber.ac.uk

Tristram David Linton Irvine-Fynn – tdi@aber.ac.uk, 01970622784, ORCiD: http://orcid.org/0000-0003-3157-6646

Thomas Owen Holt – toh08@aber.ac.uk, 01970628449, ORCiD: https://orcid.org/0000-0001-8361-0688, @tom_holt

John Paul Pryderi Jones – deri@djaweb.co.uk, 01654702001, @deri_jones

Stephen Tooth – set@aber.ac.uk, 01970622361, ORCiD: https://orcid.org/0000-0001-5714-2606

Hywel Griffiths – hmg@aber.ac.uk, 09170622674, ORCiD: https://orcid.org/0000-0002-0480-2014, @HywelGriffiths

Bryn Hubbard – byh@aber.ac.uk, 01970622783, ORCiD: https://orcid.org/0000-0002-3565-3875, @Bryn_Hubbard

Word count – 9426

Knickpoint evolution in a supraglacial stream

Despite numerous studies of knickpoints in bedrock and alluvial channels, no detailed description of knickpoint change on ice has been reported to date. This paper presents the first investigation of knickpoint evolution within a supraglacial stream. Repeat longitudinal profile surveys of a knickpoint on Vadrec del Forno, Switzerland reveal a step height increase of 115 mm and upstream migration of 0.26 m over three days during the 2017 ablation season. Rates and magnitudes of erosion vary spatially across the knickpoint in relation to differing discharge regimes. At high discharges (~ 0.013 $m^3 s^{-1}$), erosion is focused at the step base; at low discharges (~ 0.003 $m^3 s^{-1}$), erosion is focused on the reach upstream of the knickpoint, at the step lip and the step-riser face. This results in replacement of knickpoint morphology, driven by frictional thermal erosion and hydraulic action. Pool formation further influences step morphology, inducing secondary circulation and increased melt at the base of the step-riser, causing steepening. Results highlight the complexities of water flow over knickpoints, demonstrating that the stream power law does not accurately characterise changing knickpoint morphology or predict retreat rates. Although morphological similarities have been reported between supraglacial and bedrock/alluvial channels, knickpoints in non-ice-walled channels will not necessarily respond to discharge similarly to those in ice due to the different erosion processes involved.

Keywords: knickpoint; step; supraglacial; evolution; hydrodynamics; discharge

1. Introduction

Knickpoints are commonly observed features in the longitudinal profile of river channel systems. The term ‘knickpoint’ refers to channel reaches that exhibit a marked change in bed slope, and is used herein to refer to an individual step, comprising the local point of abrupt gradient change (the step lip) and the downstream channel-spanning steep segment (the 'step-riser'; Chartrand and Whiting 2000). Such changes in slope have been attributed to alterations in sediment supply (Brush and Wolman 1960) and base-level change resulting from eustatic, geological or tectonic perturbations (Haviv et al. 2010), with their presence increasing hydraulic resistance and dissipating energy (Leopold et al. 1960; Abrahams et al. 1995; Curran and Wohl 2003; Wilcox et al. 2011). Most knickpoints undergo upstream migration, governing wider landscape changes through alteration of hillslope base level (Tucker and Whipple 2002; Bigi et al. 2006; Whittaker and Boulton 2012). Three types of knickpoint retreat have been identified by Gardner (1983) using flume experiments in cohesive, homogenous substrates: (i) *parallel retreat* with retention of the original step morphology; (ii) *replacement* with alteration of the original step morphology arising from erosion above the knickpoint lip and over the step face; and (iii) *backward rotation* of the step towards the general channel slope, causing the step-riser inclination to decrease. As adjustments in bedrock/alluvial channels typically occur over decadal-to-millennial timescales, direct observations of upstream knickpoint retreat are limited. Attempts have been made to predict knickpoint retreat rates in some landscapes using the stream power incision model (Bishop et al. 2005; Crosby and Whipple 2006; Berlin and Anderson 2007; Lague 2014). This model relates knickpoint retreat rate to catchment drainage size, which acts as a proxy for discharge (Whipple and Tucker 1999; Crosby and Whipple 2006), assuming a constant flow regime. The stream power model, however, typically fails to predict observations of knickpoint retreat due to poor characterisation of changing flow regimes over a step (Dust and Wohl 2012), and the lack of consideration of sediment transport processes (Jansen et al. 2011), the role of bedrock structure (Mackey et al. 2014), plunge-pool dynamics (Scheingross and Lamb 2017) and the self-regulation of channel geometry (Baynes et al. 2018).

Within bedrock channels, there is a lack of empirical data describing actively migrating knickpoints (Cook et al. 2013), due to the typically slow retreat rates and difficulties in identifying and isolating controlling intrinsic and extrinsic factors (Kephart 2013). Knickpoint evolution mechanisms, therefore, remain poorly understood despite laboratory and flume studies investigating drivers of change (e.g. Bennet et al. 2000; Grimaud et al. 2015; Lamb et al. 2015; Baynes et al. 2018). However, knickpoint features have also been described in supraglacial (e.g. Knighton 1981, 1985; Carver et al. 1994; St Germain and Moorman 2016) and englacial channels (e.g. Pulina 1984; Holmlund 1988; Griselin 1992; Vatne 2001; Piccini et al. 2002; Vatne and Refsnes 2003; Vatne and Irvine-Fynn 2016), where their formation is considered to be related to intrinsic flow dynamics, in contrast to extrinsic factors commonly cited for bedrock/alluvial systems (Phillips et al. 2010; Yokokawa et al. 2016). This gives rise to a unique field environment that allows for isolation of hydrodynamic variables, since ice-walled streams are typically devoid of sediment load (Leopold et al. 1960; Kostrzewski and Zwoliñski 1995; Karlstrom et al. 2013), and channel boundaries are close to the melting point. These factors enable assessment of knickpoint evolution over shorter (hourly-to-diurnal) timescales. Supraglacial streams are often considered to be analogous to bedrock channels, due to their similarities in morphology and adjustment (Ewing 1970; Marston 1983; Knighton 1985; Karlstrom et al. 2013) and, thus, supraglacial investigations have been used to gain a better empirical understanding of channel formation and evolution (Ferguson 1973). Constraining supraglacial knickpoint evolution also has implications for understanding englacial drainage systems, at least where conduits exist at atmospheric pressure, owing to knickpoints forming a major component of vertical channel incision (Gulley et al. 2009; Vatne and Irvine-Fynn 2016) and, thereby, underpinning meltwater transfer to a glacier's ice-bed interface.

Currently, the potential of the supraglacial environment for examining knickpoint formation and evolution processes has not yet been fulfilled. The majority of field-based research on supraglacial streams was published several decades ago (e.g. Ewing 1970; Pinchack 1972; Dozier 1974; Hambrey 1977), and focused on hydraulic geometry (e.g. Park 1981; Marston 1983; Kostrzewski and Zwoliñski 1995; Brykała 1999) or meandering (e.g. Knighton 1972; Ferguson 1973). Although the presence of knickpoints has been reported (Dozier 1974), the only study to address this morphology in any detail examined its role in inducing pulsating flow (St Germain and Moorman 2016). Despite a recent resurgence of interest in supraglacial drainage, studies have predominantly used remotely sensed data (e.g. Joughin et al. 2013; Lampkin and VanderBerg 2014; Rippin et al. 2015; Smith et al. 2015; Karlstrom and Yang 2016; Yang et al. 2016) and, thus, do not account for a process-level understanding of local hydraulics. Therefore, there is a need to elucidate the processes responsible for morphological drainage evolution through field-based research (Gleason et al. 2016), and to advance existing numerical models (e.g. Karlstrom et al. 2013; Mantelli et al. 2015).

Here, we present repeat geometric measurements of a knickpoint within a supraglacial stream on Vadrec del Forno, Switzerland, to characterise its morphological evolution in response to hydrodynamic forcing. Measurement took place over three days during the 2017 ablation season. The results provide the first description and quantification of changing knickpoint morphology on ice, and yield insight into the varying spatial focus of hydrological erosion at differing discharges.

2. Field site

Vadrec del Forno is a 4.5 km long, temperate, Alpine valley glacier located in the Bregaglia Range of Graubünden, southeast Switzerland (46°17'N, 9°40'E; Figure 1A). The glacier flows north from the Italian border, comprising two accumulation basins that form a shallow gradient, ~ 500 m wide tongue. The glacier elevation extended from ~ 2250 to 3200 m.a.s.l in 2016, covering an area of 5 km^2. Across the ablation area, the predominant structural glaciological feature is longitudinal foliation (Jennings et al. 2014), exerting a strong control over surface meltwater drainage (cf. Hambrey 1977). This gives rise to relatively straight rills and streams flowing parallel to the glacier flow direction, providing an excellent site for examining hydrodynamics in straight channels unaffected by meander-induced secondary water circulation.

2.1 Channel reach and knickpoint characteristics

A straight 4.5 m long reach of a perennial stream containing a single transverse knickpoint was selected for investigation on the west side of the ablation zone, ~ 0.85 km from the terminus (Figure 1). Glaciologically, perennial streams are channels that persist and are repeatedly reoccupied over inter-annual timescales, in contrast to annual streams that form and melt out each year (Ewing 1970). Perennial streams, especially on non-temperate glaciers, can seed the formation of englacial channels existing at atmospheric pressure (Gulley et al. 2009), therefore, providing a better analogue for englacial drainage than annual streams. Here, the selected reach was chosen for the presence of a knickpoint in isolation, with the absence of any distinct elevation changes that may have influenced knickpoint evolution. This stream was a distributary, bifurcating from a main channel 9 m above the reach, and appeared to exploit the downglacier oriented longitudinal foliation. The reach had a low gradient (7°) and sinuosity (1.005), and ranged in width from 0.14 to 0.66 m. Despite evidence of several transverse clear ice bands cutting across the channel upstream of the knickpoint, there was negligible transverse structural variability at, or downstream of the knickpoint, suggestive of a homogenous substrate underlying the step itself, allowing patterns and rates of change to be attributed to hydrodynamic variables. Although clastic debris was visible embedded in the channel bed (Figure 1B), the stream flow was devoid of sediment bed load, with little to no transportation of ice crystals over the measurement period.

The knickpoint was classified as a 'break-in-gradient' knickpoint type (after Haviv et al. 2010), characterised by a gentle step lip and riser face with a channel-bed-supported sloping jet (Figure 1C). Over the measurement period, this knickpoint accounted for between 15 and 32 % of the 0.68 m decrease in elevation along the longitudinal profile of the stream reach. Initially, no pooling of water at the step base was observed; instead, a reverse bed slope was recorded downstream of the knickpoint with detachment of flow from the channel bed and water aeration at the downstream end of this reverse slope.

[Figure 1 near here]

3. Methods

Data was collected in the early ablation season, between, and inclusive of, the 6th and 9th July 2017. This short measurement period arose from considerable water flow reduction over the knickpoint on the 9th July, as a result of upstream flow capture. Knickpoint and channel cross-section measurements were completed between 08:00 and 12:00 before peak diurnal discharge, with the exception of the 6th July when measurements were taken between 14:00 and 15:30 and excluded cross-section geometry. Using the assumption that peak discharge has the greatest impact on changing channel morphology (Marston 1983; Carver et al. 1994), geometric measurements are considered to reflect adjustments resulting from the previous day's hydrodynamic forcing. Adjustment was assessed between each day's measurements, giving three full days of change monitoring.

3.1 Knickpoint and channel geometry

To measure knickpoint geometry, the majority of water flow over the step was temporarily diverted to the main channel upstream of the reach, using sealed water-filled bags stacked at the distributary diffluence. Water flow was diverted for ~ 20 minutes each day between 08:50 and 09:30. Once achieved, the horizontal distance of the step lip from a fixed reference point was measured to determine upstream knickpoint recession. Daily central longitudinal profiles of the step-riser were recorded using a contour gauge shaping tool, similar to techniques used for quantifying surface roughness (McCarroll and Nesje 1996). The gauge maintains the shape of a surface once moulded to it, allowing for replication with a quantified accuracy of 11 mm. Careful gauge positioning onto laminated millimetre graph paper enabled tracing of the lowermost edge using a whiteboard marker pen, with nadir photography using a 14-mpx Fujifilm Finepix JV200 digital camera allowing for extraction of profile coordinates. These profile coordinates were digitally plotted at centimetre resolution, using a Bezier spline interpolation to represent the step-riser (accurate to 5 mm).

Channel cross-section geometry was measured upstream and downstream of the knickpoint lip, to quantify vertical incision (Figure 1). Measurements were conducted from fixed reference points, established on the east stream bank. From these points, vertical depth measurements to the nearest 10 mm were recorded at 0.1 m intervals across the channel, relative to a taut tape measure anchored on the opposite bank. Vertical depth measurements and the 0.1 m measurement intervals were trigonometrically corrected to a horizontal plane, using the tape angle measured with a compass clinometer to ± 1°, with depth adjustment to the daily glacier surface elevation. The inevitable tape sag led to an uncertainty (C_{catenary}) that was quantified following Uren and Price (2005):

$$C_{\mathrm{catenary}} = \frac{w^2 D^3 (cos2\theta)}{24T^2}$$

(Equation 1)

where w is weight per unit length of tape, D is tape length, θ is the vertical angle between end-points and T is applied tension. Assuming modest tension of 10 N, (following Irvine-Fynn et al. (2014a)), for a tape length of 1.8 m and weight per unit length of 0.18 N m^{-1}, the maximum uncertainty was 1 mm. Within the horizontal plane, inevitable positional uncertainty in repeat surveys arises from ablation at the fixed reference points; however, this error is acceptable here, as cross-sections are not directly compared in absolute space.

Bank full stage is unlikely within perennial supraglacial streams, as their existence depends on incision outpacing ablation, at least initially (Knighton 1981; Marston 1983).

Therefore, flow geometry dimensions of the ‘active channel’ (width, mean channel depth below the ice surface) were derived using water height at the channel thalweg (stage) at 10:00. This ‘active channel’ denotes the area that adjusts in relation to actively flowing water (Osterkamp and Hedman 1977), providing the best approximation of channel dimensions when the channel is most stable prior to peak discharge. Daily incision rates were determined using the difference between mean cross-section depths.

3.2 Streamflow dynamics

Stream discharge was measured at hourly intervals between 09:30 and 13:30. Following Hudson and Fraser (2002), discharge (Q) was estimated using salt dilution gauging:

$$Q = \frac{k\,M}{(T_2 - T_1) \times (EC - EC_{bkgd})}$$

(Equation 2)

where M is mass of salt added in grams (here, 10 g pre-dissolved salt injected 11 m upstream of the detection point); $T_2 - T_1$ is tracer passage duration in seconds; $EC - EC_{bkgd}$ is mean electrical conductivity during the tracer passage, as measured with a REED SD-4307 conductivity meter (0.1 µS resolution, accurate to ± 2 % (REED 2015)); and k is the temperature-corrected proportionality constant, calculated as 1.5909 for 0 °C. Over the observed temperature range of 0.01 – 0.3 °C, variation in k was less than 1 % and negligible for discharge calculations. Measurements characterised the rising limb and beginning of the falling limb of diurnal discharge and, thus, captured daily peak discharge between 11:30 and 12:30. An additional discharge reading was taken on the 6th July at 15:00, while it was not possible to derive discharge on the 9th July, as flow was too low to measure.

Flow velocity along the reach was calculated from the salt tracer travel time over the thalweg distance and, following Knighton (1998), used with measurements of stage and flow width to calculate Froude and Reynolds numbers (Fr and Re, respectively). Daily maximum stream power per unit length over the knickpoint was estimated using the mean step gradient and peak discharge. Detailed observations were also made regarding the nature of water flow over the knickpoint, including defining the contact between the water and step-riser and evidence of hydraulic jumps, backpooling and splashing of water in relation to the channel morphology.

3.3 Meteorological data

In the absence of meteorological data at the glacier surface, hourly air temperature data over the measurement period were obtained from the nearest MeteoSwiss automatic weather station, located in Vicosoprano, 7 km from Vadrec del Forno. To interpolate these data to the local air temperature at the study site, a relationship describing the lapse rate between Vicosoprano and Vadrec del Forno was used, based on data from a HOBOware® weather station that had been installed on the ice during July 2016. The calculated lapse rate ($r^2 = 0.72$, $p \leq 0.01$) was -0.009 °C m^{-1}, giving a difference of 10.85 °C between the sites that was used to adjust the 2017 air temperature data. Hourly potential incident radiation at the glacier surface was calculated following Irvine-Fynn et al. (2014b).

4. Results

4.1 Knickpoint evolution

The step lip migrated upstream by 0.26 m over three days from its initial 6th July position (Figure 2), with the step-riser face steepening by 17°. Knickpoint recession rates were variable, increasing from 0.01 m day^{-1} (6th - 7th July) to 0.08 m day^{-1} (7th - 8th July), with the greatest recession of 0.17 m day^{-1} occurring between the 8th and 9th July, coincident with the greatest change in step gradient (Table 1).

Step height increased by 115 mm with the greatest change of 88 mm occurring between the 7th and 8th July. Between the 8th and 9th July, step height decreased by 18 mm. The reverse bed slope at the step base was replaced with the formation of a pool towards midday on the 8th July, with evidence of a hydraulic jump and backpooling.

[Figure 2 near here]

[Table 1 near here]

4.2 Cross-section evolution

Measured cross-sections (Figure 3) show that above the knickpoint, the channel was generally wider and shallower than below the knickpoint. Over the measurement period, mean channel depth above the knickpoint was 0.40 m, and 0.52 m below the knickpoint. The nature and rates of morphological change were variable over both space and time, with disparity between the cross-sections. Above the knickpoint, the channel cross-section was initially approximately trapezoidal (Figure 3A; 7th July). This cross-section incised by 27 mm, developing a more rounded, quasi-elliptical morphology (Figure 3A; 8th July), which further incised by 83 mm and narrowed by 160 mm to form a more triangular morphology (Figure 3A; 9th July). Below the knickpoint (Figure 3B), the channel maintained an approximately triangular cross-section, with a stable width (Table 1) and incision of 73 mm over the first two days (6th - 7th, 7th - 8th July). This profile subsequently widened by 80 mm and incised by 20 mm (8th - 9th July).

The channel upstream of the knickpoint incised 18 mm more than that below, with the majority of vertical incision occurring between the 8th and 9th July above the step, and between the 7th and 8th July below the step (Table 1; cross-section mean depths). However, the greatest change in width was recorded between the 8th and 9th July for both cross-sections. As a result, deepening and narrowing of the upstream cross-section coincided with a decrease in incision and widening of the downstream cross-section.

[Figure 3 near here]

4.3 Streamflow dynamics

Over the measurement period, discharge generally decreased (Table 1), with peak discharge on the 8th July being an order of magnitude lower than on previous days, and water flow on the 9th July being too low to measure. Water temperatures correlated positively with discharge ($r = 0.83$, $n = 11$, $p \leq 0.01$). Expectedly, discharge also correlated positively with velocity ($r = 0.82$, $n = 11$, $p \leq 0.01$) and stream power ($r = 0.99$, $n = 11$, $p < 0.01$) and, thus, stream power was significantly lower on the 8th July than on previous days ($p \leq 0.01$). The reduced discharge (8th and 9th July) was the result of upstream water capture, due to the main channel incising at a faster rate than the studied distributary reach. However, linear regressions between discharge and stream power with knickpoint retreat were not significant ($p > 0.05$).

Water flow over the knickpoint was continuously channel-bed-supported, with only occasional observations of decoupled flow for a few seconds at a time. Water flow above and below the knickpoint was mainly subcritical ($Fr < 1$) and was predominantly turbulent on the 6th and 7th July (high Re), with transitional flow on the 8th July (Table 1). As water neared the step base, lateral flow interaction with the channel banks resulted in water being diverted upwards and back towards the channel centre, causing flow convergence here and at the beginning of the reverse bed slope. A submerged impinging jet was observed at the step base. Downstream of the knickpoint, flow detachment from the channel bed occurred as the reverse bed slope deflected water upward, causing visible aeration and spraying of the channel banks. Immediately prior to midday on the 8th July, the effects of the reverse bed slope were less obvious and a hydraulic jump was present at the step base, with evidence of backpooling.

5. Discussion

5.1 Hydrodynamic forcing

In the absence of an appreciable bed load, it is reasonable to assume that erosive forces are predominantly hydrodynamic, with hydraulic action and melting driving supraglacial channel change (Knighton 1981; Marston 1983; Kostrzewski and Zwoliñski 1995; Isenko et al. 2005). However, the results demonstrate that increased retreat rate was not associated with rising discharge and stream power per unit length. This supports suggestions that the relationship between discharge and knickpoint retreat rate is oversimplified (Baynes et al. 2018). Instead, the results here show that greater knickpoint retreat occurred at lower discharges. The changing step morphology indicates non-uniformity of erosion across the step, demonstrating the complex interaction between discharge regime and knickpoint evolution (see Section 5.2). Additionally, these data further demonstrate that the simplistic stream power incision model is unlikely to adequately characterise retreating knickpoints (Howard et al. 1994; Scheingross and Lamb 2017). This supports the work of St Germain and Moorman (2016), which demonstrated that supraglacial step-pool morphologies do not necessarily form at high discharge, contrary to assumptions by Vatne and Refsnes (2003) who regard high discharge as a necessary factor for step formation in ice. Furthermore, this challenges the assumption that the greatest channel change occurs at peak discharges in ice-walled channels (Marston 1983; Carver et al. 1994), highlighting the need for measurements at increased temporal resolution to better constrain the timing and rates of evolution.

As erosion reflects the balance between driving and resisting forces (Wohl 1998; Hayakawa and Matsukura 2003), the role of ice substrate resistance in controlling knickpoint migration rates must also be considered. The channel substrate comprised clear and bubbly ice types, the former of which experiences preferential water erosion (Ewing 1970; Hambrey 1977), as exemplified by the undulating bed form troughs concordant with clear ice structures upstream of the knickpoint (Figure 1B). The observed alternation in ice types through these bed forms, had they extended downstream, could have explained the relative stability of the step lip between the 6th and 7th July, with the subsequent increase in retreat rate being the result of headward migration through clear ice to less resistant, bubbly ice upstream. However, the absence of such structural features proximate to the knickpoint indicated a homogenous substrate here, reflected by knickpoint migration via replacement. This implies that knickpoint evolution was not structurally controlled during the measurement period, supporting the argument that hydrodynamic forcing plays the dominant role in governing supraglacial step evolution.

Within an ice-walled channel, thermal erosion is an additional contributing driver of knickpoint retreat. Such heat energy transfer arises from several sources: sensible air temperature and solar radiation, friction at the water-ice interface and turbulence-induced friction within the water (Ewing 1970; Ferguson 1973; Marston 1983). Additional erosion can arise from direct channel bed ablation through shallow water columns (Holmes 1955; Dozier 1974). Although direct ablation may have been possible in this study, given the maximum recorded water depth of 0.1 m, this is not supported by the insignificant linear regression between daily mean potential incident radiation and incision rates ($r = 0.027$, $p > 0.05$). Using the ‘Enter method’, a multiple linear regression ($R^2 = 0.62$) demonstrates that discharge was the only significant predictor of water temperature ($r = 0.75$, $p < 0.05$). This indicates that frictional heat generated from viscous flow dissipation is the main component of thermal erosion in this study, supporting research by Ferguson (1973), Parker (1975) and Marston (1983) who estimated that this can account for 50 – 75 % of incision. The overall slope of the stream reach here was 7°, with that of the knickpoint face being a minimum of 18°. As Pinchack (1972) reported a requisite channel gradient of 11° to induce melt in a slightly wider stream than reported here, this indicates that frictional heat potentially plays more of a role in erosion locally, thereby contributing to knickpoint evolution.

5.2 Hydrological controls on supraglacial knickpoint evolution

The notion that knickpoint retreat rate is primarily controlled by discharge (Seidl and Dietrich 1992; Howard et al. 1994; Bishop et al. 2005) is challenged by the supraglacial stream data presented here. The greatest step retreat, gradient change and rate of upstream incision (Cross-section A) were associated with low discharges, and the greatest increase in step height and rate of downstream incision (Cross-section B) were associated with high discharges. To explain these spatial and temporal variations, we propose a conceptual model of process-morphology linkages to identify the hydrological controls on supraglacial knickpoint evolution, whereby varying discharge regimes control spatial zones of erosion over the step-riser and lead to pool formation (Figure 4). Three morphologically distinct zones of erosion are identified, with differential rates and magnitudes of change at the step lip, riser face and step base giving rise to knickpoint evolution via replacement of step morphology (Gardner 1983).

At turbulent, high discharges, (here, 6th and 7th July), vertical incision is focused at the step base. The reduced boundary resistance at high flows means that the impinging jet retains energy over the step lip and face (Marston 1983; Wilcox and Wohl 2006; Comiti et al. 2009), therefore, imparting greater hydraulic force to the step base. However, as the channel bed and step face were not smoothly polished, channel roughness elements were limited to microscale features, indicating that reduced boundary resistance is likely to have a negligible impact on energy retention. At the step base, higher water temperatures associated with turbulence are more likely to contribute to vertical incision, aided by the high degree of interaction between the water jet and the channel bed. Incision rates at the step base exceed those at the lip, leading to an increase in step height. Consequently, the knickpoint experiences considerable steepening, which contradicts the more often observed backward rotation of the knickpoint in homogenous bedrock and alluvial settings (Holland and Pickup 1976; Gardner 1983; Stein and Julien 1993; Frankel et al. 2007).

[Figure 4 near here]

At low discharges with transitional flow, (here, 8th and 9th July), erosion is focused on the reach immediately upstream of the knickpoint, the step lip and the step-riser face. At low water depths, the microscale channel roughness has a greater influence on frictional energy dissipation, increasing boundary resistance and resulting in accelerated melting of the bed upstream of the step, and at the step lip where shear stress is highest (Gardner 1983). The lower velocities associated with lower discharges act to increase the energy transfer time and, thus, enhance melt at a given point (Thorsness and Hanratty 1979), with low turbulence inhibiting energy dissipation within the flow itself. This occurs mainly above the step lip, where water flow is slower than across the step-riser as a result of the gentler slope. Additionally, enhanced erosion above the step lip is attributed to over-steepening (drawdown) of the water surface profile as flow starts to accelerate over the increasing gradient (Gardner 1983; Haviv et al. 2006; Berlin and Anderson 2009). This enhanced energy transfer reduces the stream power of the bed-supported jet (Chin 2003), resulting in less available energy to hydraulically erode the step base and causing a decrease in step height.

The finding that low discharge has a dominant control on knickpoint migration necessitates consideration of the potential methodological impact of temporary stream diversion during low flows. The magnitude of knickpoint and channel adjustment was in the order of centimetres to decimetres over 24 hours, with peak diurnal discharge only exceeding 0.009 $m^3 s^{-1}$ for a maximum of 3.5 hours over the measurement period. Low flow conditions of < 0.007 $m^3 s^{-1}$ were recorded throughout the rest of the day, with flow diversion for 20 minutes accounting for < 2 % of this time, assuming continuous 24 hour flow. Consequently, we suggest that flow diversion over such a short period had negligible impact on knickpoint evolution; however, a portion of low flow channel adjustment may have been overlooked, albeit small, as a result of this diversion. The estimated maximum discharge diverted to the main channel (~ 0.005 $m^3 s^{-1}$) is not expected to have resulted in a marked change in incision rate or eventual channel capture over the timescales involved.

5.2.1 Hydrological controls on pool development

The lack of ice structural control over observed knickpoint evolution suggests that downstream pool development on the 8th July was primarily controlled by step morphology adjustment in response to discharge variations. Using the conceptual model described in Figure 4, an explanation for pool formation can be proposed. At high discharges, localised erosion at the step base leads to over-deepening. Water pools in this depression at low discharges, with the reverse bed slope acting to further impede downstream flow. As pool development starts to reduce the effect of the impinging jet on the channel bed (Wu and Rajaratnam 1998; Zimmermann and Church 2001; Carling et al. 2005), the increased tailwater depth inhibits vertical incision and results in a predominance of lateral erosion. In our study, this is demonstrated by the coincident decrease in channel depth and increase in width below the knickpoint between the 8th and 9th July. The pooled water creates a persistent contact with the ice forming the lower section of the step-riser, causing erosion here (Figure 4), and resulting in continued and accelerated steepening of the face at low discharge. Turbulent secondary circulation back towards the step face and the formation of a hydraulic jump close to the step base enhances this erosional zone. Pool development herein appears to conform morphologically to the conceptual model proposed by Scheingross et al. (2017) to describe abrasive plunge-pool evolution in homogenous bedrock. This suggests that in a homogenous ice substrate and, even in the absence of sediment load, knickpoint retreat may be driven by vertical drilling, a knickpoint migration process described by Howard et al. (1994) and Lamb et al. (2007). This contrasts with classic waterfall erosion models that indicate knickpoint migration owing to overlying caprock failure, following removal of an underlying substrate (e.g. Gilbert 1890; Holland and Pickup 1976; Frankel et al. 2007). However, the lack of undercutting herein may be due to the reduced discharge following pool formation, with accelerated erosion of the upstream pool wall only being plausible in the case of continued flow.

Although substrate characteristics influence the shape and recession rate of knickpoints (Gardner 1983; Larue 2008; Phillips and Desloges 2014), our proposed model builds on the concept that a mutual interaction exists between the shape of the heat transfer surface and the variation in rates of heat transfer, the latter of which is determined by flow characteristics (Gilpin et al. 1980). This advances the work of Vatne and Irvine-Fynn (2016), whose insights from englacial knickpoint morphology indicated that step shape controls the type of water jet and, thus, the location of energy expenditure and heat transfer across the knickpoint face. Our model demonstrates that differing discharge regimes govern the location of erosion, a concept that can be extended to knickpoint evolution in bedrock (Carling et al. 2005) and cohesive sediment (Bennet et al. 2000), where varying degrees of surface erosion in relation to hydrological forcing have also been recorded. However, the difference in erosive mechanisms between supraglacial and bedrock/alluvial channels indicates that this model is not applicable within the latter for determining the ways in which knickpoint morphology will adjust in response to discharge alterations. Contrary to some previous assertions (e.g. Ewing 1970; Marston 1983; Knighton 1985), this shows that the systems are not analogous to one another, warranting further investigation into the differences between each environment and the processes causing the formation and adjustment of similar channel morphologies.

5.3 Interactions between morphology and flow variability

The zones of erosion outlined in Section 5.2 govern step and channel shape, and demonstrate the effect of flow dynamics on knickpoint morphology. However, channel morphology also controls flow dynamics over a step (e.g. Knighton 1981; Kostrzewski and Zwoliñski 1995; Milzow et al. 2006), determining these erosional zones. Here, this is exemplified by channel narrowing over the knickpoint, confining water flow over the step-riser and resulting in water overturning towards the channel centre with consequent flow convergence. This, in turn, gives rise to the narrow cross-section at the step base, with water concentration driving vertical incision. This feedback between channel morphology and hydraulics is complex, making it difficult to identify clear cause-and-effect relationships (Wilcox et al. 2011).

In order to determine the importance of the erosional zones outlined here in controlling knickpoint morphology and recession rates, knickpoint evolution was modelled (Figure 5) using the daily ice melt rate as an equivalent erosional process for the stream power incision model. Channel incision rates were derived from daily mean water temperature and velocity, using relationships described in Isenko et al. (2005)'s Figure 2. Each knickpoint profile was divided into linear millimetre-to-centimetre length segments based on changes in gradient using Rhino3D® software (Robert McNeel & Associates 2017), with application of calculated daily incision rates perpendicular to the local slope of each segment. Perpendicular offsetting of each segment reflected changes in the horizontal and vertical plane, and better characterised knickpoint retreat and morphological adjustment. A manually digitised curve joined the offset segments to create a full modelled profile (Figure 5). As discharge prior to 08:00 was consistently low (< 0.005 $m^3 s^{-1}$), it is assumed that stream flow is also low in the evening and negligible overnight. This assumption is supported by the high snow line position in July 2017, akin to that typically seen in late summer (Beat Kühnis, personal communication, July 2017). Snowpack depletion reduces potential water storage at the glacier surface, the volume of delayed runoff and the lag-time between peak melt and supraglacial discharge (see Willis et al. 2002). Here, the contribution of delayed runoff following peak ablation is likely to be minimal, indicating that the stream did not experience continuous water flow over a 24-hour period. Therefore, incision rates were applied for an 18-hour period to represent a maximum estimate of change, as the mean water temperatures and velocities used encompassed the rising limb and peak diurnal measurements.

[Figure 5 near here]

Comparison of the modelled profiles with observed knickpoint evolution emphasise discrepancies between both the shape and rate of evolution (Figure 5). Modelled profiles retained the original step morphology, overestimating vertical lowering (6th - 7th, 8th - 9th July) and both overestimating (6th - 7th July) and underestimating headward recession at the step lip (7th - 8th, 8th - 9th July). The inability of the model to accurately predict knickpoint evolution on ice is likely due to the assumption of constant water temperature and velocity along the profile. As the results herein demonstrate that differential zones of erosion arise at differing discharges, this suggests that use of a constant-rate melt model for characterising step evolution is too simplistic, similar to the stream power laws applied in bedrock/alluvial streams. The complexities of changing flow dynamics across a knickpoint on ice must be further investigated, to allow incorporation of these parameters and their feedback with the channel boundary into numerical models.

6. Conclusions

Until now, there has been a limited process-level understanding of knickpoint evolution within ice-walled channels, despite their importance in supraglacial and englacial incision processes. Our study of a supraglacial knickpoint on Vadrec del Forno, Switzerland provides the first detailed dataset of supraglacial knickpoint morphological change at a fine temporal resolution. The results showed recession of 0.26 m over three days, with variable rates and magnitudes of change, both spatially across the knickpoint and temporally over diurnal timescales. Low flow rates coincided with the greatest step retreat, gradient change and rate of upstream incision, and high flow rates coincided with the greatest increase in step height and rate of downstream incision. Our conceptual model proposes that discharge variations control the zones of erosion over the knickpoint, with low discharge focusing erosion on the reach upstream of the knickpoint, the step lip and step-riser face, and high discharge focusing erosion at the knickpoint base. Channel over-deepening at the knickpoint base led to pool formation, with the increased tailwater depth inhibiting vertical incision and causing lateral erosion. This confirms non-uniform water flow over the step, resulting in evolution through replacement of morphology. Bed load absence within the stream indicates the hydrodynamic nature of evolution, with the driving forces of hydraulic action and frictional thermal erosion governing morphological change. The results indicate that peak discharge may not play as dominant a role in drainage development on ice as previously considered, suggesting that the majority of morphological adjustment in features such as knickpoints may occur prior to or following high meltwater fluxes, either at a diurnal (supraglacial) or seasonal (englacial) scale.

The data presented here demonstrate that the relationships between discharge, stream power and knickpoint retreat rate commonly used in bedrock/alluvial channels fails to capture the intricacies and feedbacks of erosion processes driving knickpoint recession in ice-walled channels. Our findings show that the considerable differences in erosive mechanisms between supraglacial and bedrock/alluvial channels are likely to result in disparities in knickpoint morphological adjustment in response to varying discharge regimes. The conceptual model proposed herein has been developed from a relatively time-limited dataset, meaning that ascertaining whether results provide a relevant representation of knickpoint evolution is challenging. In order to test the wider application of the model, additional research within supraglacial environments is required at a range of spatial scales, taking into consideration channels of varying sizes, gradients and discharges. In particular, further investigation of knickpoint erosion mechanisms in relation to variable flow regimes is essential, through increasing the *temporal* and *spatial* resolution of flow measurements above, across and below knickpoints.

Acknowledgements

This work was supported by a Knowledge Economy Skills Scholarship (KESS II) under Project AU10003, a pan-Wales higher-level skills initiative led by Bangor University on behalf of the HE sector in Wales. It is part-funded by the Welsh Government's European Social Fund (ESF) convergence programme for West Wales and the Valleys. Funding was awarded to TDLI-F and JEK, with support from Deri Jones & Associates Ltd. Additional support was gratefully received from the Aberystwyth University Research Fund "ASPECT" under Grant number 12104 awarded to TDLI-F, Aberystwyth University Research Fund under Grant number 12465 awarded to TOH and TDLI-F, and the Royal Geographical Society Small Research Grant under Grant number SRG8/16 awarded to TOH. All authors recognise additional support from Aberystwyth University (DGES). MeteoSwiss are acknowledged for the provision of automatic weather station data. Emily Stratton, Ed Roberts, Sarah Easter, Nathan Daverson and Charlotte Day are all thanked for their support in the field. Edwin Baynes is thanked for initial discussions regarding the research nature and data collection, and for an informal review of the original manuscript, and helpful comments were also gratefully received from Emily Parker. The constructive comments from two anonymous reviewers are gratefully acknowledged.

Disclosure statement

No potential conflict of interest was reported by the authors.

Notes on contributors

JEK is a PhD student in Glaciology at the Centre for Glaciology, Aberystwyth University. Her main area of research is glacier drainage morphology.

TDLI-F is a Senior Lecturer in Geography at Aberystwyth University. His main area of research is glacial hydrology, which includes the hydraulics of the near-surface ice, the seasonal development of ice surface roughness and albedo, and glacier surface microbial processes.

TOH is a Lecturer in Geography at Aberystwyth University, specialising in glaciology and remote sensing. His research focuses on the use of optical, radar and microwave imagery and data to quantify changes in the cryosphere.

JPPJ is an engineering consultant and surveyor specialising in marine design and laser scanning for Deri Jones & Associates Ltd. His work focuses on the design of construction systems for large structures, and on capturing 3D information for complex man-made and natural structures.

ST is a Professor of Geography at Aberystwyth University. His main areas of research include fluvial geomorphology and sedimentology, with a particular focus on bedrock and alluvial rivers in drylands.

HMG is a Senior Lecturer in Geography at Aberystwyth University. His main areas of research include processes and rates of change in fluvial systems and reconstructing flood histories using geomorphological and documentary methods.

BH is a Professor of Geography at Aberystwyth University. His main areas of research include the links between subglacial drainage and ice motion, structural glaciology and glacier-like forms on Mars.

Author contributions

JEK and TDLI-F developed the research question and context; JEK designed and conducted the research; JEK analysed and interpreted the data, and wrote the paper with guidance from TDLI-F; TOH provided UAV imagery of the field site. All authors edited and revised the paper.

References

Abrahams AD, Li G, Atkinson JF. 1995. Step-pool streams: Adjustment to maximum flow resistance. Water Resour Res. 31(10):2593-2602.

Baynes ER, Lague D, Attal M, Gangloff A, Kirstein LA, Dugmore AJ. 2018. River self-organisation inhibits discharge control on waterfall migration. Sci Rep. 8(1):2444.

Bennet SJ, Robinson KM, Simon A, Hanson GJ. 2000. Stable knickpoints formed in cohesive sediment. Joint Conference on Water Resource Engineering and Water Resources Planning and Management; 30th July - August 2nd; Minneapolis, MN.

Berlin MM, Anderson RS. 2007. Modeling of knickpoint retreat on the Roan Plateau, western Colorado. J Geophys Res Earth Surf. 112(F3).

Berlin MM, Anderson RS. 2009. Steepened channels upstream of knickpoints: Controls on relict landscape response. J Geophys Res Earth Surf. 114(F03018).

Bigi A, Hasbargen LE, Montanari A, Paola C. 2006. Knickpoints and hillslope failures: Interactions in a steady-state experimental landscape. Special Papers Geological Society of America. 398:295-307.

Bishop P, Hoey TB, Jansen JD, Artza IL. 2005. Knickpoint recession rate and catchment area: the case of uplifted rivers in Eastern Scotland. Earth Surf Processes Landforms. 30(6):767-778.

Brush JLM, Wolman GM. 1960. Knickpoint behavior in noncohesive material: a laboratory study. Geol Soc Am Bull. 71(1):59-74.

Brykała D. 1999. Hydraulic geometry of a supraglacial stream on the Waldemar Glacier (Spitsbergen) in the summer of 1997. Polish Polar Studies: 26th International Polar Symposium; June 1999; Lublin, Poland. p. 51-64.

Carling P, Tych W, Richardson K. 2005. The hydraulic scaling of step-pool systems. River, Coastal and Estuarine Morphodynamics. New York: Taylor & Francis; p. 55-63.

Carver S, Sear D, Valentine E. 1994. An observation of roll waves in a supraglacial meltwater channel, Harlech Gletscher, East Greenland. J Glaciol. 40(134):75-78.

Chartrand SM, Whiting PJ. 2000. Alluvial architecture in headwater streams with special emphasis on step-pool topography. Earth Surf Processes Landforms. 25(6):583-600.

Chin A. 2003. The geomorphic significance of step–pools in mountain streams. Geomorphology. 55(1-4):125-137.

Comiti F, Cadol D, Wohl EE. 2009. Flow regimes, bed morphology, and flow resistance in self-formed step-pool channels. Water Resour Res. 45(4):W04424.

Cook KL, Turowski JM, Hovius N. 2013. A demonstration of the importance of bedload transport for fluvial bedrock erosion and knickpoint propagation. Earth Surf Processes Landforms. 38(7):683-695.

Crosby BT, Whipple KX. 2006. Knickpoint initiation and distribution within fluvial networks: 236 waterfalls in the Waipaoa River, North Island, New Zealand. Geomorphology. 82(1-2):16-38.

Curran JH, Wohl EE. 2003. Large woody debris and flow resistance in step-pool channels, Cascade Range, Washington. Geomorphology. 51(1-3):141-157.

Dozier J. 1974. Channel adjustments in supraglacial streams. Icefield Ranges Research Project, Scientific Results. 4:189-205.

Dust D, Wohl E. 2012. Characterization of the hydraulics at natural step crests in step-pool streams via weir flow concepts. Water Resour Res. 48(W09542).

Ewing KJ. 1970. Supraglacial streams on the Kaskawulsh Glacier, Yukon Territory. Arctic Institute of North America Research paper. 57:121-167.

Ferguson RI. 1973. Sinuosity of supraglacial streams. Geol Soc Am Bull. 84(1):251-256.

Frankel KL, Pazzaglia FJ, Vaughn JD. 2007. Knickpoint evolution in a vertically bedded substrate, upstream-dipping terraces, and Atlantic slope bedrock channels. Geol Soc Am Bull. 119(3-4):476-486.

Gardner TW. 1983. Experimental study of knickpoint and longitudinal profile evolution in cohesive, homogenous material. Geol Soc Am Bull. 94(5):664-672.

Gilbert G. 1890. The history of the Niagara River: extracted from the sixth annual report to the Commissioners of the State Reservation at Niagara, for the year 1889. Albany, NY.

Gilpin R, Hirata T, Cheng K. 1980. Wave formation and heat transfer at an ice-water interface in the presence of a turbulent flow. J Fluid Mech. 99(3):619-640.

Gleason CJ, Smith LC, Chu VW, Legleiter CJ, Pitcher LH, Overstreet BT, Rennermalm AK, Forster RR, Yang K. 2016. Characterizing supraglacial meltwater channel hydraulics on the Greenland Ice Sheet from in situ observations. Earth Surf Processes Landforms. 41(14):2111-2122.

Grimaud J-L, Paola C, Voller V. 2015. Experimental migration of knickpoints: influence of style of base-level fall and bed lithology. Earth Surf Dyn. 3(3):11-23.

Griselin M. 1992. In the depth of a small polar glacier (Loven East Glacier, Spitsbergen). Proceedings of the 2nd International GLACKIPR Symposium; 10-16 February; University of Silesia, Poland. p. 51-63.

Gulley JD, Benn DI, Müller D, Luckman A. 2009. A cut-and-closure origin for englacial conduits in uncrevassed regions of polythermal glaciers. J Glaciol. 55(189):66-80.

Hambrey MJ. 1977. Supraglacial drainage and its relationship to structure, with particular reference to Charles Rabots Bre, Okstindan, Norway. Norsk Geografisk Tidsskrift. 31(2):69-77.

Haviv I, Enzel Y, Whipple K, Zilberman E, Matmon A, Stone J, Fifield K. 2010. Evolution of vertical knickpoints (waterfalls) with resistant caprock: Insights from numerical modeling. J Geophys Res F: Earth Surf. 115(F03028).

Haviv I, Enzel Y, Whipple KX, Zilberman E, Stone J, Matmon A, Fifield LK. 2006. Amplified erosion above waterfalls and oversteepened bedrock reaches. J Geophys Res F: Earth Surf. 111(F04004).

Hayakawa Y, Matsukura Y. 2003. Recession rates of waterfalls in Boso Peninsula, Japan, and a predictive equation. Earth Surf Processes Landforms. 28(6):675-684.

Holland W, Pickup G. 1976. Flume study of knickpoint development in stratified sediment. Geol Soc Am Bull. 87(1):76-82.

Holmes GW. 1955. Morphology and hydrology of the Mint Julep area, Southwest Greenland. Alabama, US: Air University. Mint Julep Reports., Part II: A-104-B.

Holmlund P. 1988. Internal geometry and evolution of moulins, Storglaciären, Sweden. J Glaciol. 34(117):242-248.

Howard AD, Dietrich WE, Seidl MA. 1994. Modeling fluvial erosion on regional to continental scales. J Geophys Res B: Solid Earth. 99(B7):13971-13986.

Hudson R, Fraser J. 2002. Alternative methods of flow rating in small coastal streams. BC, Canada: Forest Service British Columbia. EN-014.

Irvine-Fynn TDL, Sanz-Ablanedo E, Rutter N, Smith MW, Chandler JH. 2014a. Measuring glacier surface roughness using plot-scale, close-range digital photogrammetry. J Glaciol. 60(223):957-969.

Irvine-Fynn TDL, Hanna E, Barrand N, Porter P, Kohler J, Hodson A. 2014b. Examination of a physically based, high-resolution, distributed Arctic temperature-index melt model, on Midtre Lovénbreen, Svalbard. Hydrol Processes. 28(1):134-149.

Isenko E, Naruse R, Mavlyudov B. 2005. Water temperature in englacial and supraglacial channels: Change along the flow and contribution to ice melting on the channel wall. Cold Reg Sci Technol. 42(1):53-62.

Jansen JD, Fabel D, Bishop P, Xu S, Schnabel C, Codilean AT. 2011. Does decreasing paraglacial sediment supply slow knickpoint retreat? Geology. 39(6):543-546.

Jennings SJ, Hambrey MJ, Glasser NF. 2014. Ice flow-unit influence on glacier structure, debris entrainment and transport. Earth Surf Processes Landforms. 39(10):1279-1292.

Joughin I, Das SB, Flowers G, Behn MD, Alley RB, King MA, Smith B, Bamber JL, van den Broeke MR, Van Angelen J. 2013. Influence of ice-sheet geometry and supraglacial lakes on seasonal ice-flow variability. The Cryosphere. 7(4):1185-1192.

Karlstrom L, Gajjar P, Manga M. 2013. Meander formation in supraglacial streams. J Geophys Res Earth Surf. 118(3):1897-1907.

Karlstrom L, Yang K. 2016. Fluvial supraglacial landscape evolution on the Greenland Ice Sheet. Geophys Res Lett. 43(6):2683-2692.

Kephart CW. 2013. Flow and geometry measurements at an active knickpoint [Master's thesis]. Lincoln: University of Nebraska.

Knighton AD. 1972. Meandering habit of supraglacial streams. Geol Soc Am Bull. 83(1):201-204.

Knighton AD. 1981. Channel form and flow characteristics of supraglacial streams, Austre Okstindbreen, Norway. Arct Alp Res. 13(3):295-306.

Knighton AD. 1985. Channel form adjustment in supraglacial streams, Austre Okstindbreen, Norway. Arct Alp Res. 17(4):451-466.

Knighton AD. 1998. Fluvial Forms and Processes. London: Hodder Arnold.

Kostrzewski A, Zwoliñski Z. 1995. Hydraulic geometry of a supraglacial stream. Quaestiones Geographicae. [accessed 11/05/2018]:[165-176 p.]. http://www.staff.amu.edu.pl/~zbzw/gh/gh1.htm.

Lague D. 2014. The stream power river incision model: evidence, theory and beyond. Earth Surf Processes Landforms. 39(1):38-61.

Lamb MP, Finnegan NJ, Scheingross JS, Sklar LS. 2015. New insights into the mechanics of fluvial bedrock erosion through flume experiments and theory. Geomorphology. 244:33-55.

Lamb MP, Howard AD, Dietrich WE, Perron JT. 2007. Formation of amphitheater-headed valleys by waterfall erosion after large-scale slumping on Hawai'i. Geol Soc Am Bull. 119(7-8):805-822.

Lampkin D, VanderBerg J. 2014. Supraglacial melt channel networks in the Jakobshavn Isbræ region during the 2007 melt season. Hydrol Processes. 28(25):6038-6053.

Larue J-P. 2008. Effects of tectonics and lithology on long profiles of 16 rivers of the southern Central Massif border between the Aude and the Orb (France). Geomorphology. 93(3-4):343-367.

Leopold LB, Bagnold RA, Wolman MG, Brush JLM. 1960. Flow resistance in sinuous or irregular channels. Washington, D.C.: Geological Survey Professional Paper. 282-D:111.

Mackey BH, Scheingross JS, Lamb MP, Farley KA. 2014. Knickpoint formation, rapid propagation, and landscape response following coastal cliff retreat at the last interglacial sea-level highstand: Kaua'i, Hawai'i. Geol Soc Am Bull. 126(7-8):925-942.

Mantelli E, Camporeale C, Ridolfi L. 2015. Supraglacial channel inception: Modeling and processes. Water Resour Res. 51(9):7044-7063.

Marston RA. 1983. Supraglacial stream dynamics on the Juneau Icefield. Ann Assoc Am Geogr. 73(4):597-608.

McCarroll D, Nesje A. 1996. Rock surface roughness as an indicator of degree of rock surface weathering. Earth Surf Processes Landforms. 21(10):963-977.

Milzow C, Molnar P, McArdell BW, Burlando P. 2006. Spatial organization in the step-pool structure of a steep mountain stream (Vogelbach, Switzerland). Water Resour Res. 42(W04418).

Osterkamp W, Hedman E. 1977. Variation of width and discharge for natural high-gradient stream channels. Water Resour Res. 13(2):256-258.

Park CC. 1981. Hydraulic geometry of a supraglacial stream: some observations from the Val d'herens, Switzerland. Revue de Géomorphologie Dynamique. 30(1):1-9.

Parker G. 1975. Meandering of supraglacial melt streams. Water Resour Res. 11(4):551-552.

Phillips JD, McCormack S, Duan J, Russo JP, Schumacher AM, Tripathi GN, Brockman RB, Mays AB, Pulugurtha S. 2010. Origin and interpretation of knickpoints in the Big South Fork River basin, Kentucky–Tennessee. Geomorphology. 114(3):188-198.

Phillips R, Desloges J. 2014. Glacially conditioned specific stream powers in low-relief river catchments of the southern Laurentian Great Lakes. Geomorphology. 206:271-287.

Piccini L, Romeo A, Badino G. 2002. Moulins and marginal contact caves in the Gornergletscher, Switzerland. Nimbus. 23-24:94-99.

Pinchack AC. 1972. Diurnal flow variations and thermal erosion in supraglacial streams. East Lansing, Michigan: Michigan State University. Technical Report 33: Part XII.

PlanetTeam. 2017. Planet Application Program Interface: In Space for Life on Earth. San Francisco, CA.

Pulina M. 1984. Glacierkarst phenomena in Spitsbergen. Norsk Geografisk Tidsskrift. 38(3-4):163-168.

REED Instruments. 2015. REED SD-4307 Salt/TDS/Conductivity Datalogger Instruction Manual. REED Instruments.

Rippin DM, Pomfret A, King N. 2015. High resolution mapping of supra-glacial drainage pathways reveals link between micro-channel drainage density, surface roughness and surface reflectance. Earth Surf Processes Landforms. 40(10):1279-1290.

Robert McNeel & Associates. 2017. Rhino3D software Version 5. Barcelona: Robert McNeel & Associates.

Scheingross JS, Lamb MP. 2017. A mechanistic model of waterfall plunge pool erosion into bedrock. J Geophys Res F: Earth Surf. 122(11):2079-2104.

Scheingross JS, Lo DY, Lamb MP. 2017. Self-formed waterfall plunge pools in homogeneous rock. Geophys Res Lett. 44(1):200-208.

Seidl M, Dietrich W. 1992. The problem of bedrock channel erosion. Catena Supplement. 23:101-124.

Smith LC, Chu VW, Yang K, Gleason CJ, Pitcher LH, Rennermalm AK, Legleiter CJ, Behar AE, Overstreet BT, Moustafa SE. 2015. Efficient meltwater drainage through supraglacial streams and rivers on the southwest Greenland Ice Sheet. Proc Natl Acad Sci USA. 112(4):1001-1006.

St Germain S, Moorman B. 2016. The development of a pulsating supraglacial stream. Ann Glaciol. 57(72):31-38.

Stein O, Julien P. 1993. Criterion delineating the mode of headcut migration. J Hydraul Eng. 119(1):37-50.

Thorsness C, Hanratty T. 1979. Mass-transfer between a flowing fluid and a solid wavy surface. AIChE Journal. 25(4):686-697.

Tucker G, Whipple K. 2002. Topographic outcomes predicted by stream erosion models: Sensitivity analysis and intermodel comparison. J Geophys Res B: Solid Earth. 107(B9).

Uren J, Price W. 2005. Surveying for engineers. 4th ed. New York: Palgrave Macmillan.

Vatne G. 2001. Geometry of englacial water conduits, Austre Brøggerbreen, Svalbard. Norsk Geografisk Tidsskrift. 55(2):85-93.

Vatne G, Irvine-Fynn TDL. 2016. Morphological dynamics of an englacial channel. Hydrol Earth Syst Sci. 20(7):2947-2964.

Vatne G, Refsnes I. 2003. Channel pattern and geometry of englacial conduits. 6th International Symposium 'Glacier caves and karst in Polar Regions'; Ny-Ålesund, Svalbard. p. 181-188.

Whipple KX, Tucker GE. 1999. Dynamics of the stream-power river incision model: Implications for height limits of mountain ranges, landscape response timescales, and research needs. J Geophys Res B: Solid Earth. 104(B8):17661-17674.

Whittaker AC, Boulton SJ. 2012. Tectonic and climatic controls on knickpoint retreat rates and landscape response times. J Geophys Res F: Earth Surf. 117(F2).

Wilcox AC, Wohl EE. 2006. Flow resistance dynamics in step-pool stream channels: 1. Large woody debris and controls on total resistance. Water Resour Res. 42(5):W05418.

Wilcox AC, Wohl EE, Comiti F, Mao L. 2011. Hydraulics, morphology, and energy dissipation in an alpine step-pool channel. Water Resour Res. 47(7):W07514.

Willis IC, Arnold NS, Brock BW. 2002. Effect of snowpack removal on energy balance, melt and runoff in a small supraglacial catchment. Hydrol Process. 16(14):2721-2749.

Wohl EE. 1998. Bedrock channel morphology in relation to erosional processes. In: Tinkler KJ, Wohl EE, editors. Rivers Over Rock: Fluvial Processes in Bedrock Channels. Washington, D.C.: American Geophysical Union; p. 133-151.

Wu S, Rajaratnam N. 1998. Impinging jet and surface flow regimes at drop. J Hydrol Res 36(1):69-74.

Yang K, Smith LC, Chu VW, Pitcher LH, Gleason CJ, Rennermalm AK, Li M. 2016. Fluvial morphometry of supraglacial river networks on the southwest Greenland Ice Sheet. GIScience & Remote Sensing. 53(4):459-482.

Yokokawa M, Izumi N, Naito K, Parker G, Yamada T, Greve R. 2016. Cyclic steps on ice. J Geophys Res Earth Surf. 121(5):1023-1048.

Zimmermann A, Church M. 2001. Channel morphology, gradient profiles and bed stresses during flood in a step–pool channel. Geomorphology. 40(3-4):311-327.

Table 1. Summary of knickpoint and cross-section dimensions, flow parameters, and general interpolated weather trends for each day.

Day	**Step height (mm)**	**Step gradient (°)**	**Cross-section above knickpoint**		**Cross-section below knickpoint**		**Peak discharge ($m^3 s^{-1}$)**	**Mean velocity ($m s^{-1}$)**	**Maximum stream power per unit length ($W m^{-1}$)**	**Mean water temperature (°C)**	**Froude number range**		**Reynolds number range**	**Mean daily air temperature (°C)**	**Mean daily potential incident radiation ($W m^{-2}$)**
			Mean depth (m)	**Width (m)**	**Mean depth (m)**	**Width (m)**					**Above knickpoint**	**Below knickpoint**			
6th July	100	18	-	-	-	-	0.013	0.75	46.81	0.3	1.08	0.76	4431	13.85	898
7th July	128	23	0.35	0.29	0.48	0.17	0.011	0.83	47.42	0.17	0.76 - 0.99	0.91 - 0.99	2836 - 6263	12.35	712
8th July	215	30	0.38	0.29	0.55	0.17	0.003	0.41	14.63	0.08	0.2 - 0.69	0.24 - 0.69	1004 - 3131	14.67	768
9th July	198	38	0.46	0.09	0.53	0.25	-	-	-	-	-	-	-	-	-

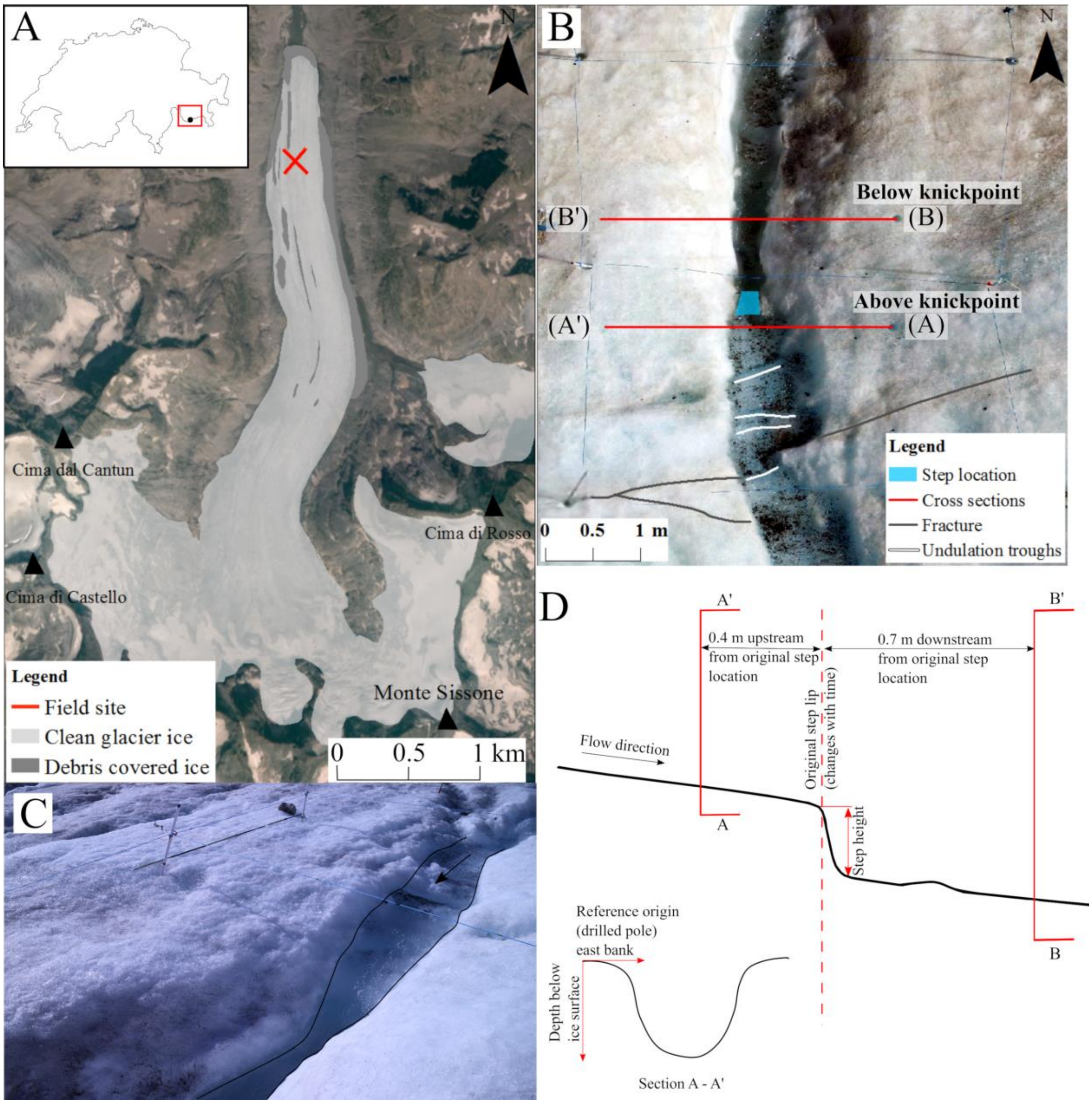

A
N
Cima dal Cantun
Cima di Rosso
Cima di Castello
Monte Sissone
Legend
Field site
Clean glacier ice
Debris covered ice
0 0.5 1 km
B
N
Below knickpoint
(B') (B)
Above knickpoint
(A') (A)
Legend
Step location
Cross sections
Fracture
Undulation troughs
0 0.5 1 m
C
D
A'
B'
0.4 m upstream from original step location
0.7 m downstream from original step location
Original step lip (changes with time)
Flow direction
Step height
A
B
Reference origin (drilled pole) east bank
Depth below ice surface
Section A - A'

Figure 1

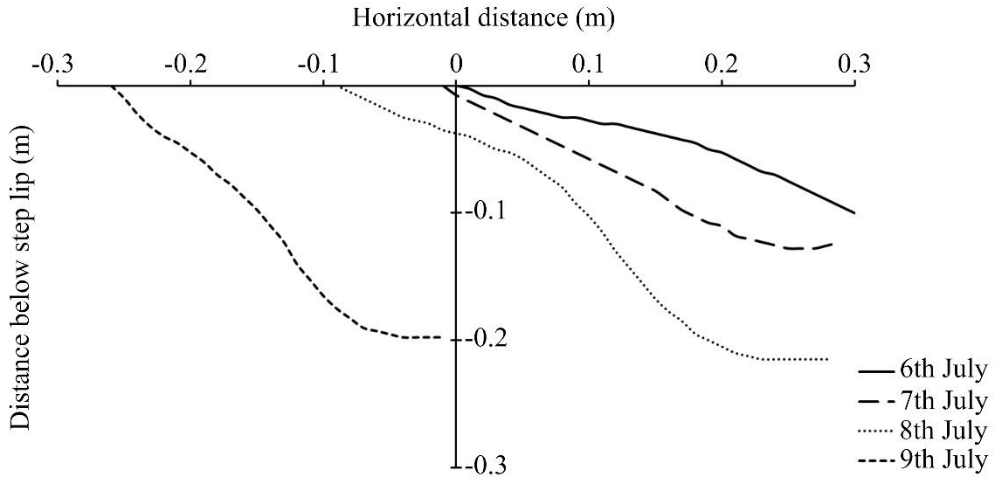

Figure 2

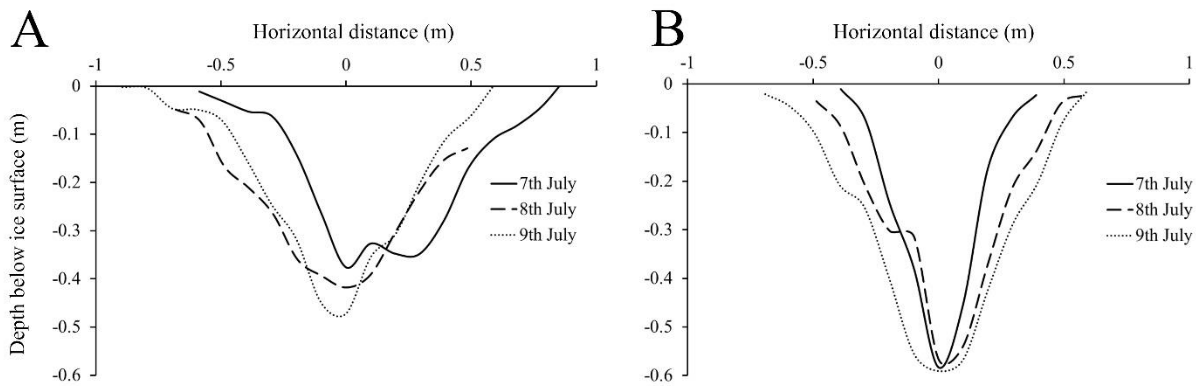

Figure 3

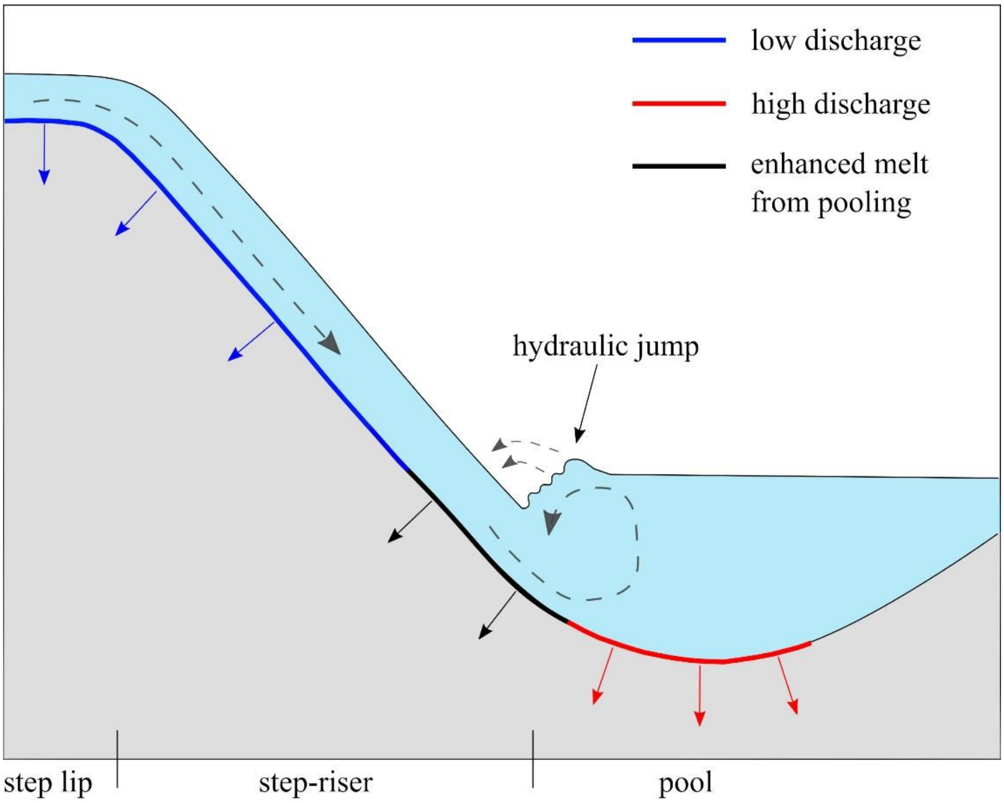

Figure 4

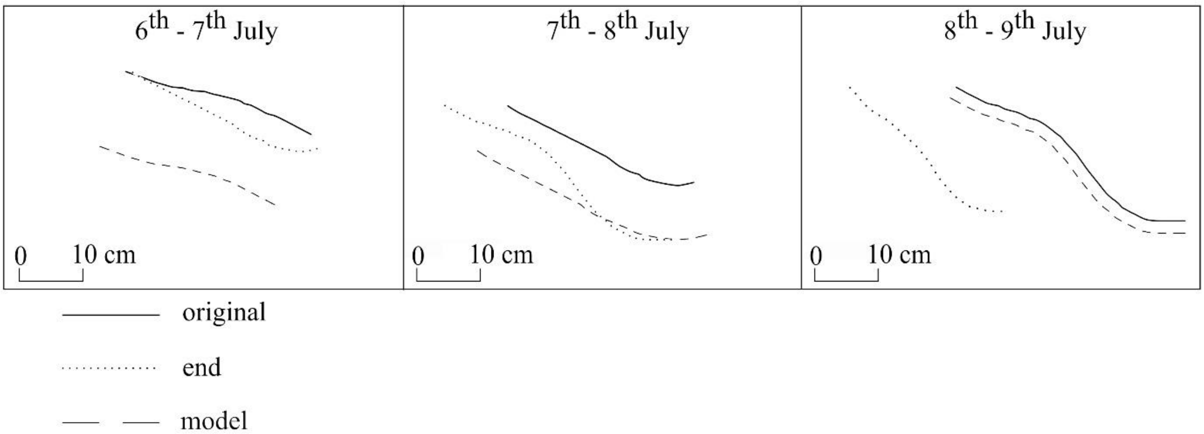

Figure 5.

Figure 1. (A) The red cross marks the field experiment location on Vadrec del Forno, with the location of the glacier within Switzerland inset. RapidEye imagery obtained from PlanetTeam (2017). (B) The stream reach planform, demonstrating the fracture and undulation troughs upstream of the knickpoint. Longitudinal foliation within the stream vicinity is oriented between 58° and 89° relative to north. Water and glacier flow is also to the north. Aerial imagery obtained from an elevation of 30 m at a resolution of 0.02 m using a DJI Phantom 3 Series Standard quadcopter. (C) The step with the direction of water flow denoted by the black arrow. The 2.3 m long crevasse probe lying horizontal on the far stream bank provides scale. (D) Schematic longitudinal profile of the knickpoint, demonstrating the locations at which cross-section geometry and step height was measured, with an example cross-section inset.

Figure 2. Central step-riser profiles for each day demonstrating the recession and morphology of the step face immediately downstream of the step lip. The graph origin denotes the location of the original step lip (6th July). To facilitate direct comparison, profiles have not been corrected for vertical lowering.

Figure 3. Channel cross-sections measured on different days illustrating changes above (A) and below (B) the knickpoint. The direction of flow is into the page. Cross-sections are geometrically accurate relative to the glacier surface at the time of measurement, with the x-axis denoting lateral distance from the thalweg.

Figure 4. Schematic illustration of the differing zones of erosion across the knickpoint at varying discharges. The solid arrows denote the direction of boundary erosion and the dashed arrows denote the direction of water flow.

Figure 5. Observed and modelled knickpoint evolution for each day, showing the original knickpoint profile (as recorded on the start date), the end profile (as recorded on the end date) and the modelled profile derived from 18-hour melt rates.